# FRACTURE OF ANCHORS IN ROCK

**A. Fathy, J. Planas, M. Elices y G.V. Guinea**

**Departamento de Ciencia de Materiales de la Universidad Politécnica de Madrid.**
**E. T. S de Ingenieros de Caminos, Canales y Puertos.**
**Ciudad Universitaria s/n, 28040-Madrid.**

**Resumen.** Este artículo analiza el problema, propuesto por el RILEM Technical Committee 90, de un anclaje en tensión plana en una placa de material casi-fragil. El problema se abordó experimentalmente mediante ensayos de anclajes en placas de granito. Se consideraron varios tamaños y luces de carga para conseguir un cuadro completo del comportamiento. Se usó la simulación numérica de fractura elástica lineal (FEL) mediante el programa interactivo de elementos finitos FRANC© para conseguir una primera interpretación del comportamiento observado. Los resultados muestran, como se esperaba, que la FEL no puede predecir con exactitud las cargas máximas, excepto para tamaños grandes, y que para ello se necesitan modelos más realistas. Sin embargo el análisis también indica que esta geometría es frágil y que el comportamiento está mucho más próximo a la FEL que al estado límite de agotamiento plástico. Para este tipo de geometría, tanto la FEL como los resultados experimentales indican que la fractura tiende a producirse a lo largo de una única fisura bilateral aproximadamente perpendicular al eje de carga. El mecanismo de fractura para esta probeta bidimensional y relativamente esbelta no es nunca cónico, y la extrapolación a situaciones tridimensionales es inútil. El análisis numérico basado en FEL es capaz de predecir las trayectorias de las fisuras siempre que se establezcan adecuadamente las condiciones de contorno, que resultan ser no lineales.

**Abstract.** This paper analyzes the problem, proposed by RILEM Technical Committee 90, of a plane stress anchor in a quasi-brittle material. The problem was tackled experimentally by testing anchors in granite plates. To achieve a complete picture of the behaviour, various sizes and loading spans were considered. Numerical simulation using linear elastic fracture mechanics (LEFM) and the interactive finite element code FRANC© were used to get the first rough interpretation of the observed behaviour. The results show, as expected, that LEFM cannot accurately predict peak loads, except for the largest sizes, and more realistic models are needed for such purposes. However, the analysis also shows that this is a brittle geometry, and the behaviour is much closer to LEFM than to limit analysis. For this type of geometry, both LEFM computations and experimental measurements indicate that failure tends to be through a single bilateral crack roughly perpendicular to the load axis. The failure mechanism of this slender two dimensional 2D model is never conical, and extrapolation to 3D axisymmetric pull-out tests is useless. Numerical analysis based on LEFM is able to predict crack trajectories provided the boundary conditions —which turn out to be nonlinear— are properly stated.

## 1. INTRODUCTION

The analysis of the strength of anchor bolts embedded in concrete and rock has received great attention in the last decade, as is shown by the RILEM activity in this field [1-3]. In particular, the application of fracture mechanics techniques to predict rupture loads is under consideration. In this paper, an experimental study and an initial theoretical analysis are presented for the case of a plane stress geometry for a steel anchor bolt in a granite plate. Several sizes with different supporting distances were tested and analyzed.

After presenting the experimental and numerical methodology in sections 2 and 3, a comparison of the experimental results and of the LEFM predictions are undertaken in section 4. It is shown that nonlinear fracture theories must be considered if the behaviour, particularly the size effect behaviour, is to be accurately predicted, and that the results may be sensitive to precise boundary conditions

The more detailed analysis presented in section 5 shows that this is indeed the case. It also shows that the crack path may be very well approximated by LEFM, provided that the actual boundary conditions are brought into play. The essential conclusions are summarized in section 6, closing the paper.

## 2. EXPERIMENTAL WORK

The geometry of the plane-stress problem given by RILEM is depicted in Fig. 1. Pull-out test specimens were scaled up to four anchor depths $d$= 30, 50, 75 and 150 mm in order to study the size effect phenomenon. Three loading spans were investigated, corresponding to $a=d/2$, $d$ and $2d$.

Rectangular plates were cut using a water-cooled diamond saw from a single commercial granite plate 30 mm thick. To avoid bias due to potential material anisotropy, the orientation of the specimens was always the same. Three specimens were fabricated for each size and geometry, giving a total of 30 specimens.

The anchor opening (T shape) was made using a water-jet cutting system which resulted in a good precise opening of very high accuracy (±0.15 mm). Granite plates were machined to leave a 0.5 mm gap opening to facilitate housing process of anchors. The anchor bolts were made of steel, with a yield limit of 325 MPa.

The test set-up was carefully designed to give clear boundary conditions so as to help in numerical analysis modelling. The load bearing parts of the system (rollers, bearing plates) were scaled in accordance with specimen depth to preserve geometrical similarity.

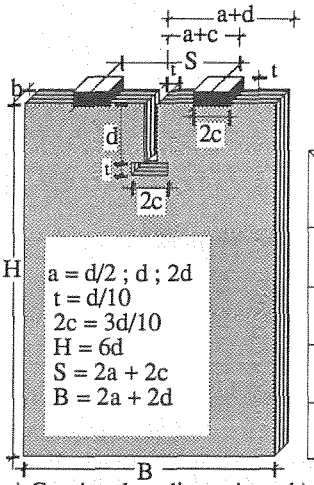


| a / d | d/2 | d | 2d |
|---|---|---|---|
| 30 | 15 | 30 | 60 |
| 50 | 25 | 50 | 100 |
| 75 | 37.5 | 75 | 150 |
| 150 | — | 150 | — |

a) Granite plate dimensions b) Selected anchor dimensions

**Fig. 1**. Specimen geometry and plate dimensions.

All tests were performed with the fixture depicted in Fig. 2, based on a hydraulic testing machine INSTRON 8501 equipped with a 25 kN capacity load-cell of better than 50 N precision. The displacement at point O, the centre of the anchor head, was measured using two displacement transducers, one on each side of the specimen, and the average of their readings was taken as a measure of the centre-line displacement δ. The strain-gauge-based transducers, manufactured in our department, are accurate to within 5 microns.

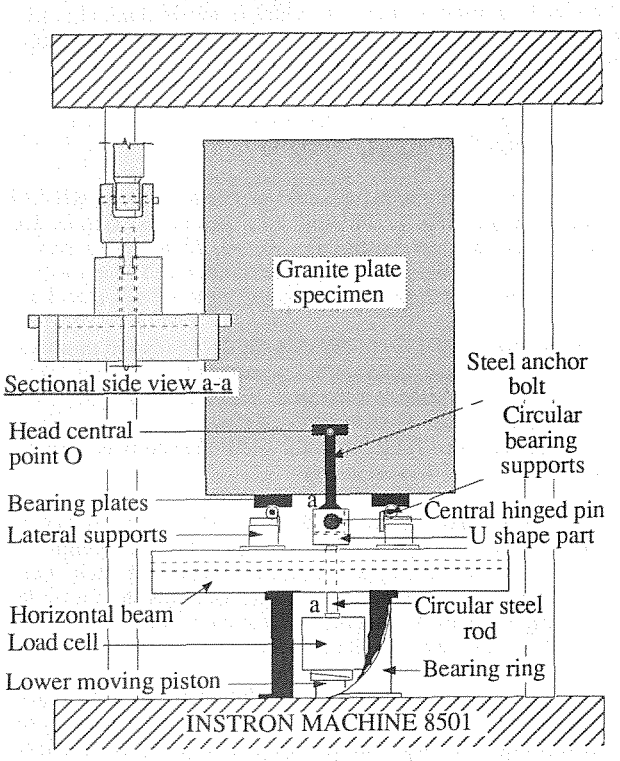


**Fig. 2**. Pull-out testing device.

The tests were performed in actuator position control, at a constant displacement rate proportional to the anchor bolt depth *d*, and the rate was chosen to reach the maximum load 3 to 5 minutes after test initiation.

The load and displacement measurements were recorded automatically using a Hewlett-Packard Data Acquisition System (DAS) composed of a VISHAY unit driven by a HP 9825 computer. Five hundred readings of the load P, the vertical displacements $\delta_1$ and $\delta_2$ were scanned and stored in a matrix of 500x3 data.

## 3. NUMERICAL ANALYSIS

The first approach to modelling the fracture of granite plates was made using linear elastic fracture mechanics (LEFM). The simulation was conducted using the finite element code FRANC© (FRacture ANalysis Code), running on a Deck Station 5000/200 [4, 5]. Although granite is thought to behave as a cohesive material rather than as linear elastic, LEFM provides useful insight into the large size limiting behaviour.

To allow LEFM calculations, a short initial crack ($\Delta a \approx 0.02\ d$) was introduced at the lower corner of the anchor housing in such a direction as to give zero mode II stress intensity factor (more precisely, $K_{II} \leq \pm\ 0.01 K_{Ic}$). As the crack propagated, the mesh was automatically rebuilt along the crack, leaving element dimensions at the crack tip unchanged. A maximum circumferential stress criterion was used to decide the cracking direction, and the increment in crack length was selected in such a way that the new crack tip was in pure mode I, $K_{II} = 0$, within the limits $K_{II} \leq \pm\ 0.03 K_{Ic}$ . The critical stress intensity factor was taken to be $K_{Ic} = 2.60$ MPa$\sqrt{m}$, obtained from the plane stress relationship $K_{Ic} = \sqrt{E G_F}$ ). At each propagation step, the load, crack mouth displacements and anchor head displacement were recorded.

The geometry and dimensions of the analyzed specimens were exactly the same as those used in the experimental tests. Four anchor depths and three support distances for $d$=50 mm were checked. The mechanical properties of the granite (measured in [6]) are summarized in Table 1. The steel support and the anchor bolt were modelled with E = 200 GPa and ν = 0.3.

**Table 1**. Mechanical properties of the granite

| Property | Mean ± Std.Dev |
|---|---|
| Young Modulus, E (GPa) | 39 ± 4 |
| Tensile Strength, $f_t$ (MPa) | 12.6 ± 1.1 |
| Fracture Energy, $G_F$ (J/m$^2$) | 173 ± 17 |

Only half of the specimen was modelled by finite elements as is shown in Fig. 3 (symmetric behaviour is assumed). The anchor was modelled in the same way and was separated from the specimen by a 0.5 mm gap except on the load transmitting area, where perfect adhesion was assumed as dictated by the RILEM description of the numerical round robin. The finite element mesh for all specimens is composed of eight-node quadrilateral elements at the initial propagation region and six-node triangular elements elsewhere, as shown in Fig 3. The system was loaded by a uniform stress at the end of the anchor shaft .

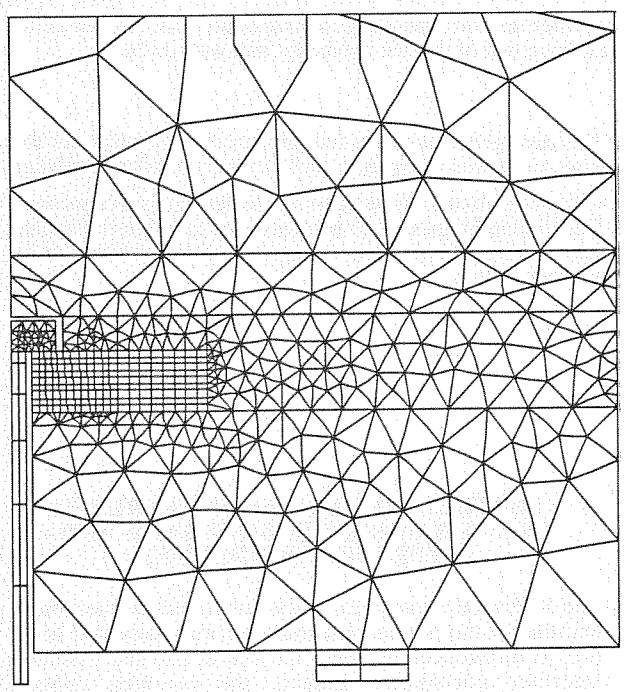

**Fig. 3**. Finite element mesh.

## 4. RESULTS

### 4.1 Peak loads and size effect

The maximum peak loads are summarized in Table 2. Experimental results indicate that the failure load is not increasing proportionally to the anchor embedded depth *d*, i.e. size effect exists. Also there is no significant change of the load when changing the support distance *a*, as frequently predicted from numerical modelling, see [3].

These results show that although the order of magnitude is captured, LEFM is unable to predict accurately the maximum loads; more involved procedures —such as cohesive models— should be used for numerical modelling.

It is worth noting that the numerical predictions deviate much more for the case *a*= *d*/2 than for the other two geometries.

**Table 2.** Maximum pull-out loads for tested anchor bolt.

| depth | Peak Load ± std dev. (kN) | | | | | |
|---|---|---|---|---|---|---|
| d | a=d/2 | | a=d | | a=2d | |
| (mm) | Exp. | Num. | Exp. | Num. | Exp. | Num. |
| 30 | 7.6± .2 | 17.0 | 6.7± .6 | 10.8 | 8.7± .7 | 10.5 |
| 50 | 9.9± .4 | 21.9 | 10.2± .7 | 13.9 | 10.5± .6 | 13.6 |
| 75 | 10.6± .9 | 26.8 | 10.3± .6 | 17.0 | 11.9± .2 | 16.7 |
| 150 | -- | -- | 22.7± .7 | 24.1 | -- | -- |

With the above results, the dimensionless log-log size effect plots of Figs. 4-6 were drawn. In these plots, the limit for very small sizes (strength of materials theory) was estimated using the rigid-perfectly plastic mechanism depicted in Fig. 7 . The LEFM solution is obtained from

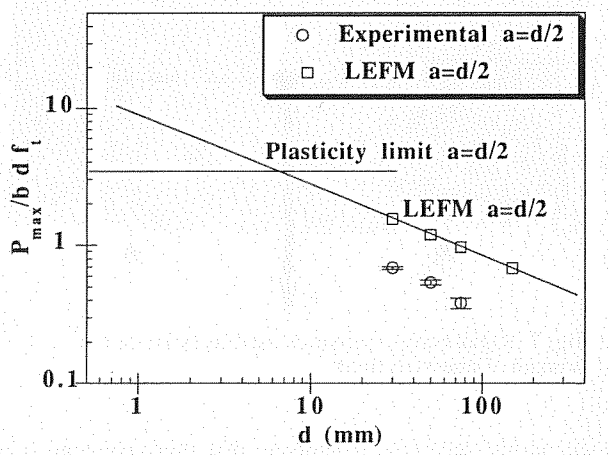


**Fig. 4**. Size effect plot for a=d/2.

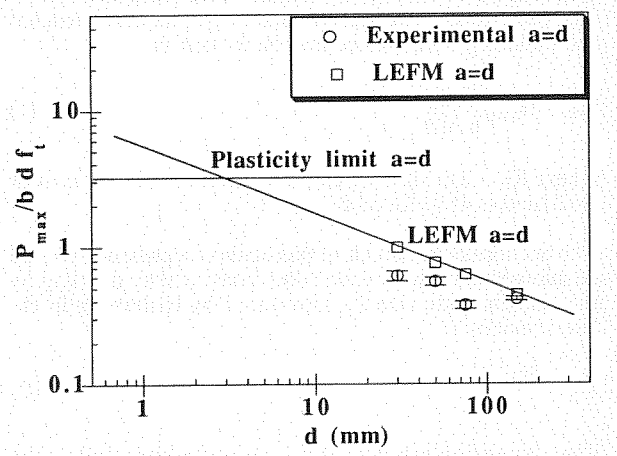


**Fig. 5**. Size effect plot for a=d.

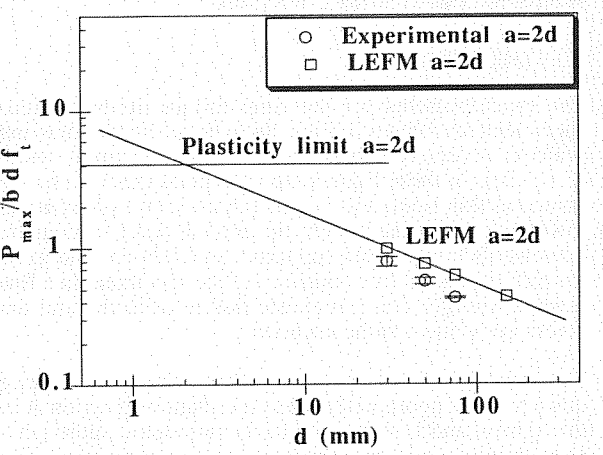


**Fig. 6**. Size effect plot for a=2d.

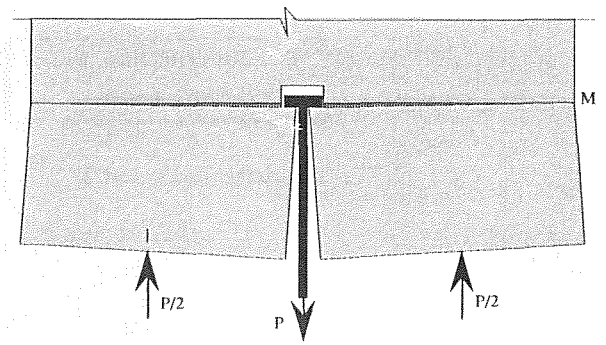


**Fig. 7.** Rigid-body kinematics used to estimate the strength of materials limit.

numerical analysis; it happens that this geometry is a negative geometry [7], which means that the stress intensity factor first decreases when the crack extends at constant load, then goes through a minimum and starts to increase. The peak load is obviously attained when the crack reaches the stationary point, which may be written as

$$K_{Ic} = \alpha_{min} \frac{P_{max}}{b\sqrt{d}} \qquad (1)$$

where $K_{Ic} = 2.6$ MPa$\sqrt{m}$ and $\alpha$ is equal to 1.25 for $a=d$ or $a=2d$ and $\alpha=0.80$ for $a=d/2$.

The anchor depth (which in this context represents the size of the specimen) was made nondimensional by dividing by the characteristic size $\ell_{ch}$ introduced by Hillerborg in the late seventies:

$$\ell_{ch} = \frac{E\,G_F}{f_t^2} \qquad (2)$$

The dimensionless size $d/\ell_{ch}$ is sometimes called the brittleness number, and is taken as an indicator of the brittleness of the structure, which, as shown in Figs. 4-6, approaches LEFM as $d/\ell_{ch}$ increases.

4.3 Crack patterns

The crack patterns for the final failure of the various specimens are shown in Figs. 8a to 8c where the drawing scale is inversely proportional to the specimen width ($2.3d+2a$). In these figures the individual crack paths are shown as thin lines, and in general are seen to start at the lower corner point under the anchor head, propagate downwards (towards the supports), and then rise and grow towards the lateral free boundary of the specimen. In a few cases a strongly non-symmetric failure occurred and the cracks grew down to the supports.

The envelope of the dominant patterns, those not running down to the support, is shown as the shadowed region A in the figures, and is seen to be fairly symmetric, although a very slight asymmetry may anyway be appreciated. The envelope of the few cracks that ran to the supports is the shadowed area B (not present in specimens with $a=d/2$), and corresponds to totally asymmetric fractures.

The numerical crack paths corresponding to LEFM prediction are represented in these figures as a thick line which is symmetric because of the symmetry enforced by the finite element modelization. The essential point is that the LEFM patterns are quite close to the average crack pattern for the dominant (quasi-symmetric) mode for the geometries corresponding to $a=d/2$ and $a=d$, but run quite far from that of the last geometry, that with $a=2d$.

This divergence of actual and predicted crack paths for the case $a=2d$ was intriguing, and further numerical analyses were performed to investigate the underlying mechanisms. This deviation appears to be due to the fact that the actual interfacial conditions are strongly nonlinear, as shown in the next section.

## 5. FURTHER NUMERICAL RESEARCH ON THE INFLUENCE OF BOUNDARY AND INTERFACE CONDITIONS

The difference between the crack path found in experiments and that of the numerical prediction was suspected to be due to differences between the actual and the assumed interface conditions. Indeed, the assumed contact conditions correspond to perfect adherence, which implies infinite friction, and very small horizontal and rotational movement on the contact area, because of the high relative stiffness of the steel. In reality, there is no adherence, but some kind of frictional contact, so that —since a gap always exists between the steel shaft and the granite— a frictional force will act at the beginning of the loading with a free horizontal movement, and later, when the horizontal movement closes the gap, the loading will proceed at a nearly fixed horizontal displacement.

To check that the above picture could match the actual behaviour, preliminary computations were performed to show that the difference between free horizontal movement and fully constrained movement was enough to explain the differences. The results of such computations are shown in Fig. 9. It appears that when no horizontal kinematic restriction exists, the crack path tends to propagate at approximately 45° right to the bottom free boundary (path ob in Fig. 9). When the horizontal displacements at the anchor head are restricted in any way, however, the path is completely different and grows nearly horizontally towards the lateral free boundary (paths oc and od in Fig.9). The experimental paths run between the above extreme cases and it is possible, in principle, to reproduce them by using non-linear mixed boundary conditions.

To see how an intermediate path may be obtained, the above hypothesized behaviour was simulated in the following very rough way: The load of the anchor bolt was concentrated in one node as depicted in Fig. 10. The three cases shown were analyzed in order to get a feeling about the implied error by concentrating the load in a single node. At the beginning of the calculation, a horizontal frictional force $X = 0.3\,P$ was assumed (constant friction equal to 0.3). The crack was then propagated under this proportional loading under a point where the horizontal gap was exhausted, and then the computation proceeded at fixed horizontal displacement of the loaded node.

The results are shown in Fig. 11 where it becomes apparent that the crack paths for the three cases (Fig. 10) show the same trend except for very short crack lengths (which may be expected from Saint Venant's principle), and that one may indeed obtain intermediate crack paths by assuming an

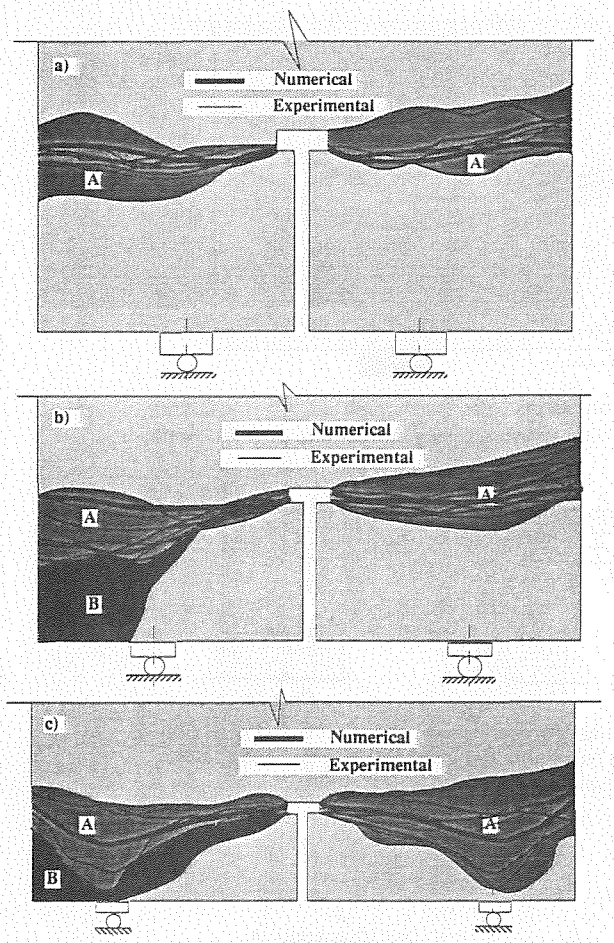


**Fig. 8**. Comparison of numerically predicted crack patterns with experimental results: a) supports at a=d/2, b) supports at a=d; c) supports at a=2d.

adequate friction coefficient and an initial gap. This fully supports the idea that the actual crack path is obtained by a mixed mechanism as described in Fig. 12, where for small displacements a frictional force exists, while for larger displacements the gap is exhausted and a horizontal bearing force appears on the granite.

## 6. CONCLUSIONS

From the above results, the following conclusions can be drawn

1. LEFM cannot accurately predict peak loads, except for the largest sizes, and more realistic models are needed for such purposes.

2 Numerical evaluation of the stress intensity factor along the crack path shows that —at constant load— it first decreases and goes through a minimum for a crack extension of about 0.1 d. This means that the geometry is negative and hence brittle, as discussed in [7]. This tendency is confirmed by the size effect plot, which shows that the experimental peak loads are much closer to LEFM than to the strength of materials limit.

3. For this type of geometry, both LEFM computations and experimental measurements indicate that failure tends to be through a single bilateral crack roughly perpendicular to the load axis. The failure mechanism of this slender 2D model is never conical and extrapolation to 3D axisymmetric pull-out tests is useless.

4. Numerical analysis based on LEFM is able to predict crack trajectories provided the boundary conditions are properly stated. Experimental crack patterns were numerically reproduced by splitting the process in a frictional initial phase, followed by a fixed displacement phase after the gap between concrete and steel is closed.

## 7. ACKNOWLEDGEMENTS

The authors thank Prof. A. Ingraffea for providing them with FRANC© and Dr. Javier Llorca for helping with computation. Financial support for this research was provided by the Comisión Interministerial de Ciencia y Tecnología, CICYT, Spain, under grant PB90-0276, and by the Polytechnic University of Madrid under grant A-91 0020 02-31.

## 8. REFERENCES

[1] RILEM TC 90-FMA, "Round-Robin Analysis of Anchor Bolts-Invitation", Materials and Structures, Vol. 23, Nº. 133, pp. 78, Jan., 1990.

[2] RILEM TC 90-FMA, "Round-Robin Analysis and Tests of Anchor Bolts-Invitation", RILEM News, 1, 1991[1].

[3] RILEM TC 90-FMA, "Round-Robin Analysis of Anchor Bolts", RILEM TC 90-FMA Fracture Mechanics of Concrete-Applications, Preliminary report, second ed., Delft, June, 1991.

[4] FRANC©, "FRacture ANalysis Code (FRANC)", Users Guide & Programmers Guide, version 2.0, Rand Hall, Cornell University, Ithaca, NewYork, February 20, 1988.

[5] FRANC©, "FRacture ANalysis Code (FRANC)", version 2.4, Rand Hall, Cornell University, Ithaca, NewYork, April, 1990.

[6] Fathy A., "Aplicación de la Mecánica de la Fractura a Rocas y Materiales Pétreos", Tesis Doctoral, Universidad Politecnica de Madrid, 1992.

[7] Planas J. and Elices M., "Anomalous Structural Size Effect in Cohesive Materials Like Concrete", in Serviceability and Durability of Construction Materials, Vol, 2, ed. B. A. Suprenant, American Society of Civil Engineers, New York, pp. 1345-1356, 1990.

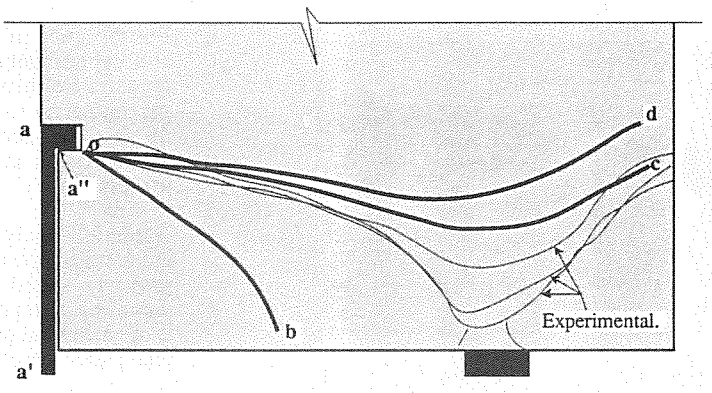


**Fig. 9.** Crack patterns for various boundary conditions. **ob:** crack path for no horizontal forces. **oc:** crack path for zero horizontal displacement along **oa''**. **od:** crack path for zero horizontal displacement along **aa'**.

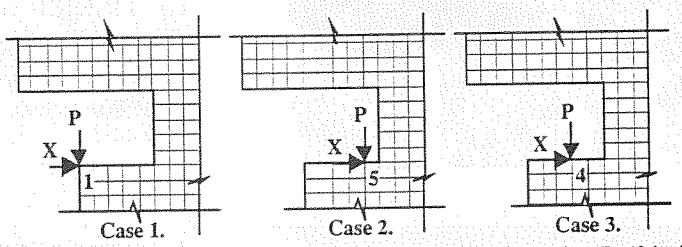


**Fig. 10**. Simplified loading cases. The horizontal force **X** is set equal to **0.3 P** (friction coefficient =0.3) until the horizontal displacement fills the initial gap between steel and granite. Subsequent loading proceeds at fixed horizontal displacement of the loaded node.

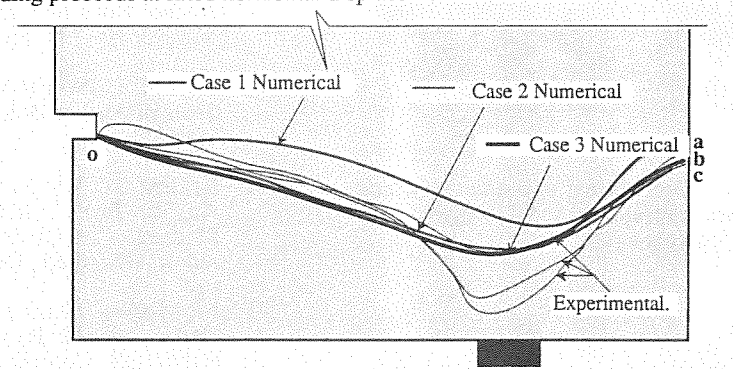


**Fig. 11**. Crack patterns for the specimens with a=150 mm, d=75 mm. The numerical loading cases correspond to those defined in Fig. 10.

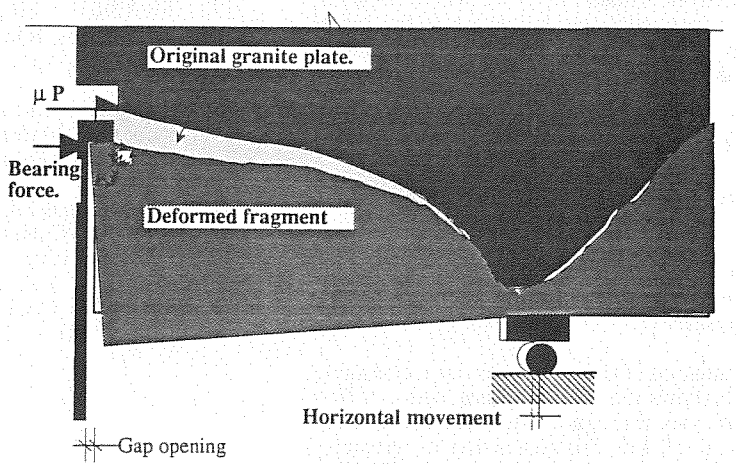


**Fig. 12**. Failure process in the pull-out plane stress problem: Initial cracking proceeds under frictional contact force **μP**, while the gap between the granite and the anchor decreases and the crack grows downwards (light grey picture). When the gap is exhausted, a horizontal bearing force appears that prevents further horizontal displacements, and the crack kinks upward (dark grey picture).